

Comparative Thermodynamic Analysis on Design Performance Characteristics of Solid Oxide Fuel Cell/Gas Turbine Hybrid Power Systems

Sung Ku Park, Won Jun Yang, Joon Hee Lee

Graduate School, Inha University,

253 Yonghyun-Dong, Nam-Gu, Incheon 402-751, Korea

Tong Seop Kim*

Department of Mechanical Engineering, Inha University,

253 Yonghyun-Dong, Nam-Gu, Incheon 402-751, Korea

This paper presents analysis results for the hybrid power system combining a solid oxide fuel cell and a gas turbine. Two system layouts, with the major difference being the operating pressure of the fuel cell, were considered and their thermodynamic design performances were compared. Critical temperature parameters affecting the design performances of the hybrid systems were considered as constraints for the system design. In addition to energy analysis, exergy analysis has been adopted to examine the performance differences depending on system layouts and design conditions. Under a relaxed temperature constraint on the cell, the ambient pressure system exhibits relatively larger power capacity but requires both higher cell temperature and temperature rise at the cell for a given gas turbine design condition. The pressurized system utilizes the high temperature gas from the fuel cell more effectively than the ambient pressure system, and thus exhibits better efficiency. Under a restricted temperature constraint on the cell, the efficiency advantage of the pressurized system becomes manifested.

Key Words : Solid Oxide Fuel Cell, Gas Turbine, Design, Ambient Pressure System, Pressurized System, Exergy Destruction

Nomenclature

AR	: Air bypass ratio	LHV	: Lower heating value [kJ/kg]
\bar{e}	: Specific exergy [kJ/kmol]	\dot{m}	: Mass flow rate [kg/s]
\dot{E}_d	: Exergy destruction rate [kW]	\dot{n}	: Molar flow rate [kmol/s]
\dot{E}_f	: Fuel exergy input rate [kW]	P	: Pressure [bar]
F	: Faraday constant [96,486 C/mol]	PWR	: Power ratio
FCT	: Fuel cell temperature [°C]	\dot{Q}	: Heat transfer rate [kW]
FR	: Additional fuel supply ratio	SCR	: Steam carbon ratio
GT	: Gas turbine	SOFC	: Solid oxide fuel cell
\bar{h}	: Molar specific enthalpy [kJ/kmol]	\bar{s}	: Molar entropy [kJ/kmolK]
I	: Current [A]	T	: Temperature [°C]
		ΔT_c	: Temperature difference at the cell [°C]
		TIT	: Turbine inlet temperature [°C]
		U	: Fuel utilization factor at the cell
		V	: Voltage [V]
		\dot{W}	: Power [kW]
		η	: Efficiency

* Corresponding Author,

E-mail : kts@inha.ac.kr

TEL : +82-32-860-7307; FAX : +82-32-868-1716

Department of Mechanical Engineering, Inha University, 253 Yonghyun-Dong, Nam-Gu, Incheon 402-751, Korea. (Manuscript Received June 1, 2006; Revised December 18, 2006)

Superscripts

<i>ch</i>	: Chemical
<i>ph</i>	: Physical

Subscripts

0	: Reference (ambient) condition
a	: Air
AC	: Alternating current
aux	: Auxiliary
C	: Compressor
c	: Cell
conv	: Conversion
DC	: Direct current
f	: Fuel
gen	: Generator
HS	: Hybrid system
i	: Composition
j	: Location
in	: Inlet
m	: Mechanical
out	: Outlet
ref	: Reformer
T	: Turbine

1. Introduction

Fuel cells have rapidly gained worldwide attention as future power sources in diverse applications. In particular, the solid oxide fuel cell is considered very suitable for the electric power plant application. One of its attractive features is its high operating temperature (600~1000°C), which allows favorable combination with a heat engine such as a gas turbine. Consequently, R&D efforts for the SOFC/GT hybrid system have been initiated worldwide and a few systems are under development for commercialization (Veyo et al., 2003 ; Agnew et al., 2005). Various system analyses have also been initiated considering diverse system configurations and design options (Liese and Gemmen, 2003 ; Song et al., 2005 ; Yang et al., 2005). Since the hybrid system combines the two sub-systems (fuel cell and gas turbine) which are totally different in principle to produce synergetic effects, the most important step in designing the entire system is the system layout design. Often, a thermodynamically optimal system design cannot be

achieved due to the difficulty in matching the sub-systems smoothly. This is also true for the hybrid system, where two totally different sub-systems are to be matched. The operating pressure of the fuel cell is one of the primary factors that affect the system layout (White, 1999). Depending on the operating pressure of the fuel cell, the system layout is classified into two cases: ambient pressure system and pressurized system.

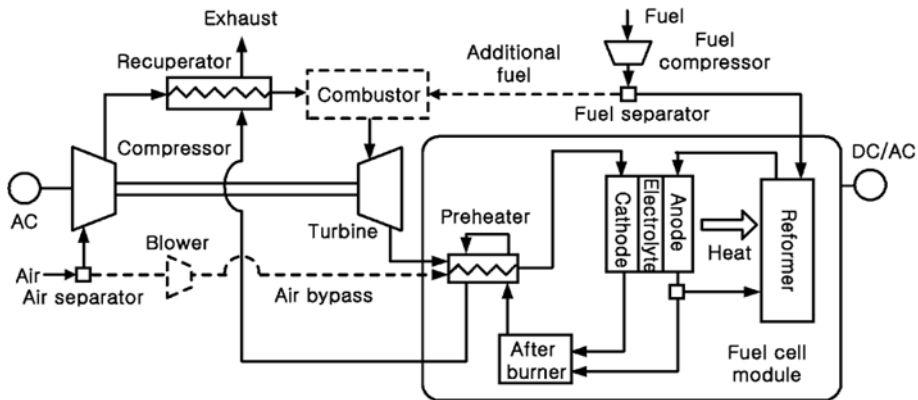
This study aims to analyze design performances of both the ambient pressure system and the pressurized system, focusing on the influence of major design parameters on the system performance. System performances are examined in terms of the design constraints on the cell, and performance limitations due to the matching of main design parameters are investigated. The design performances of the two layouts and effect of critical design constraint of the cell on the performances of both systems are the primary focus of this study. In many thermodynamic systems with diverse design variants, exergy analysis usually provides useful criteria for performance comparison. This is also true for the fuel cell/gas turbine hybrid systems as demonstrated in a few examples (Massardo and Magistri, 2001 ; Chan et al., 2002). Accordingly, exergy accounting is carried out to examine the performance differences among different system layouts and various design conditions, in detail.

2. System Layouts

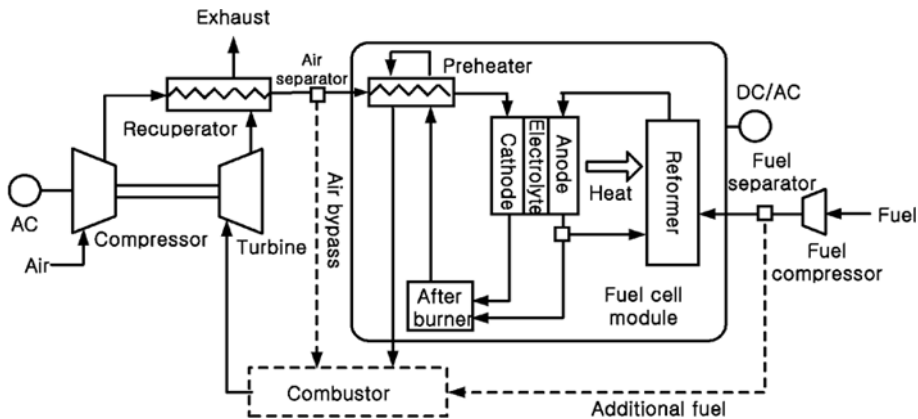
Figure 1 shows the schematics of the two SOFC/GT hybrid system layouts investigated in this study. In the ambient pressure system, the SOFC operates at a pressure close to the atmospheric pressure, driven by the gas from the gas turbine exit. In the pressurized system, pressurized air from the compressor enters the SOFC first, and then the SOFC exit gas drives the turbine. Since the fuel is natural gas, it needs to be reformed. There are various options in designing the fuel processing system (Larminie and Dicks, 2000 ; Singhal and Kendall, 2003). In this study, steam reforming is considered because its energy conversion efficiency is higher than those of the other reforming methods such as partial oxidation and autothermal reaction. It

has been adopted in most systems under commercial development (Veyo et al., 2003 ; Agnew et al., 2005). Internal reforming is considered in this study because it provides higher system efficiency than external reforming (Liese and Gemmen, 2003 ; Yang et al., 2006). The reformer is located inside the cell stack and the heat required for the endothermic reforming process is supplied from the cell stack through thermal contact. The steam for reforming is supplied by recirculating the anode exit gas, which contains sufficient steam. The recuperator recovers the exhaust heat. The preheater heats up the air (or gas) flowing into the fuel cell. In this study, the degree of preheating is regulated to meet a given temperature at the fuel cell inlet. Some of the fuel remains unreacted at the exit of the fuel cell and is combusted at the afterburner. The heat required for the preheater is supplied from the afterburner. The dotted lines denote the

additional fuel supply line and the air bypass line. Without these functions, three main design parameters (the cell inlet air temperature, the cell operating temperature and the turbine inlet temperature) can not be set independently. In that case, only two of them can be given as design inputs and the remaining parameter is obtained as a result of the design analysis as will be explained in the first part of the analysis (section 4.1). The dotted lines are required for the system designs where the three parameters are to be assigned independently as design inputs. Design performance under these restricted design constraints will be presented in the second part of the analysis (section 4.2). Since this study aims to compare design point performances among different system configurations, all cases analyzed here are considered to be independent design cases under various design requirements.



(a) Ambient pressure system

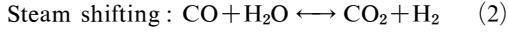
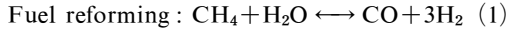


(b) Pressurized system

Fig. 1 SOFC/GT hybrid system layouts

3. Analysis

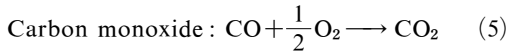
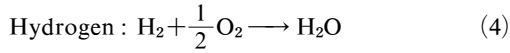
Methane, the supplied fuel, is reformed before it is supplied to the SOFC as a hydrogen-rich fuel. The following steam reforming is considered :



Equilibrium reactions are assumed. The following steam carbon ratio determines the amount of the steam supplied to the reformer.

$$SCR = \frac{\dot{n}_{\text{H}_2\text{O}}}{\dot{n}_{\text{CH}_4}} \quad (3)$$

With this value, the ratio of the recirculation flow at the anode exit is decided. Both hydrogen and carbon monoxide generated by the steam reforming process participate in the electrochemical reactions in the SOFC as follows :



The following fuel utilization factor at the cell is defined as the ratio between reacted to supplied effective fuel components at the cell :

$$U = \frac{(\dot{n}_{\text{H}_2} + \dot{n}_{\text{CO}})_{\text{reacted}}}{(\dot{n}_{\text{H}_2} + \dot{n}_{\text{CO}})_{\text{supplied}}} \quad (6)$$

The SOFC generates DC power, which is then converted into final AC power as follows :

$$\dot{W}_{\text{SOFC,DC}} = VI = V \cdot (\dot{n}_{\text{H}_2} + \dot{n}_{\text{CO}})_{\text{reacted}} \cdot 2F \quad (7)$$

$$\dot{W}_{\text{SOFC,AC}} = \dot{W}_{\text{FC,DC}} \cdot \eta_{\text{conv}} \quad (8)$$

Since the system adopts an internal reformer, heat is transferred from the cell stack to the reformer to maintain the endothermic steam reforming reaction. The following equations represent the energy balances at the cell stack and the reformer.

Cell stack :

$$\sum_{in} \dot{n}_i \bar{h}_i = \sum_{out} \dot{n}_i \bar{h}_i + \dot{W}_{\text{SOFC,DC}} + \dot{Q}_{\text{ref}} \quad (9)$$

Reformer :

$$\sum_{in} \dot{n}_i \bar{h}_i + \dot{Q}_{\text{ref}} = \sum_{out} \dot{n}_i \bar{h}_i, \text{ where } \dot{Q}_{\text{ref}} > 0 \quad (10)$$

The cell voltage is a major parameter that determines the cell performance and is usually a function of operating pressure, temperature and current density. It also depends strongly on the detailed cell material. Since this study is focused on design performance comparison, a rather simplified method is used to assign the voltage. A reasonable value of 0.7 V is assigned to a reference condition of 800°C and 3.5 bar. A correlation (Massrdo and Lubelli, 1998) provides the dependence of the cell voltage on the temperature. The current density (current per unit cell area) is assumed to be constant for all design cases. The cell voltage also depends on the operating pressure ; this relation is modeled using a published correlation (EG & G Service Parson, Inc., 2000). Consequently, the cell voltage for any condition can be predicted as a function of cell temperature and pressure. The temperatures of the both streams at the cell exit are assumed to be same as the cell operating temperature (FCT). The temperature difference (rise) at the cell is defined as follows :

$$\Delta T_c = FCT - \text{cathode inlet air temperature} \quad (11)$$

At the after burner, combustible compositions (hydrogen, carbon monoxide, methane) exiting from the anode are burned and some portion of the heat is transferred to the preheater.

The turbine supplies power to the compressor and auxiliary components, and the net gas turbine power is calculated as follows :

$$\dot{W}_{\text{GT,AC}} = (\dot{W}_T \cdot \eta_m - \dot{W}_C) \cdot \eta_{\text{gen}} - \dot{W}_{\text{aux}} \quad (12)$$

Thus, the total hybrid system power is the summation of gas turbine power and SOFC power, and the system efficiency is defined as follows :

$$\eta_{\text{HS}} = \frac{\dot{W}_{\text{HS}}}{(\dot{m} \cdot LHV)_f} \quad (13)$$

$$\text{where } \dot{W}_{\text{HS}} = \dot{W}_{\text{SOFC,AC}} + \dot{W}_{\text{GT,AC}}$$

The power ratio is defined as the ratio between the fuel cell power and the gas turbine power as follows :

$$PWR = \frac{\dot{W}_{\text{FC,AC}}}{\dot{W}_{\text{GT,AC}}} \quad (14)$$

Detailed exergy analysis is incorporated in the calculation procedure. At each flow stream, exergy per unit molar flow rate for each gas composition is defined as follows :

$$\bar{e} = \bar{e}^{ph} + \bar{e}^{ch} \quad (15)$$

The physical exergy is defined as follows :

$$\bar{e}^{ph} = \bar{h} - \bar{h}_o - T_o \cdot (\bar{s} - \bar{s}_o) \quad (16)$$

For a fuel, the chemical exergy (\bar{e}^{ch}) means the work potential due to its reaction with the ambient air. For common gas mixtures, it means the chemical potential differences between the stream and the environment. The definition and calculation of the chemical exergy may be referred to literatures (Moran and Schiuba, 1994 ; Moran and Shapiro, 2004). For each control volume (each component), the following exergy balance equation is applied to quantify the exergy destruction at the component.

$$\dot{E}_d = \sum_j \left(1 - \frac{T_o}{T_j} \right) \cdot \dot{Q}_j - W + \sum_{in} \dot{n}_i \bar{e}_i - \sum_{out} \dot{n}_i \bar{e}_i \quad (17)$$

A process analysis software (Aspen Technology, 2004), embedded with all the energy and exergy models described above, has been used for the analysis. Assumed parameters are explained here. Ambient condition is 15°C and 1atm. Fuel utilization factor is 0.7 and steam carbon ratio is 3. Characteristic parameters of micro gas turbines (small gas turbine up to 200 kW) are adopted for the gas turbine components. To represent state-of-the-art micro gas turbines, the pressure ratio of 3.5 is adopted. Isentropic efficiencies of compressor and turbine are 78% and 85%, respectively. Turbine cooling is not considered. The reference recuperator effectiveness is 0.83. This reference effectiveness is the maximum value and needs to be reduced if the temperature of the gas entering the recuperator is high enough. In the ambient pressure system, if the gas temperature is high enough, heat transfer from the exhaust gas to the recuperator should be limited to meet the given turbine inlet temperature by designing the recuperator with a reduced effectiveness. In the pressurized system, if the turbine exit gas temperature is high enough, the preheater is not requir-

ed and heat addition at the recuperator should be limited to meet the cell inlet temperature. The DC to AC conversion efficiency of the fuel cell is 93% and the mechanical efficiency and the generator efficiency of the gas turbine are 96% and 93% respectively. Since this study does not intend to confine itself to analyzing systems with fixed specifications of the SOFC and the gas turbine, constant air supply rate of 1.0 kg/s is assumed in all cases.

Two kinds of analyses have been performed. First, the cell inlet air temperature is fixed and the turbine inlet temperature is set as the main design parameter. In this case, the dotted lines in Fig. 1 are not adopted. The cell temperature is determined as a result of the analysis. Secondly, a more restricted design condition is assigned on the cell. The temperature difference (rise) at the cell is an important design parameter because it greatly affects the system performance. Examples of the relation between system performance and the temperature difference at the cell, for a pressurized SOFC hybrid system, can be found in the literature (Yang et al. 2005 ; Yang, et al. 2006). The similar result has also been found for the molten carbonate fuel cell/gas turbine hybrid systems (Oh and Kim, 2006). A greater cell temperature difference yields higher efficiency. However, this temperature difference at the cell has a strong correlation with the thermal stress evolution inside the cell and should be regulated strictly in some system configurations where it tends to increase excessively. Therefore, performance comparison based on an equivalent temperature difference at the cell for different system layouts would be more reasonable. Accordingly, the temperature difference at the cell is given as a design constraint in the second part of this study.

4. Results and Discussion

4.1 Relaxed constraint on the cell

As shown in Fig. 1, the cell inlet (cathode inlet) air temperature is satisfied by appropriate heating at the preheater. In general, there is a design range of the cell inlet temperature considering stable electrochemical reaction (Singhal and Kendall,

2003). In the analyses of this section, 700°C is adopted as a conservative value for the cell inlet temperature. The temperature difference at the cell is not constrained in this calculation, and thus, the dotted lines of Fig. 1 are not used.

Analysis results are shown in Fig. 2. The design turbine inlet temperature (TIT) ranges from 750°C to 950°C. The first figure shows the hybrid system efficiency and the required fuel cell temperature (FCT), and the second figure presents the total hybrid system power and the power ratio. Common trends for the two layouts will be examined first. In both layouts, a higher design TIT requires a higher FCT. A higher fuel cell temperature means that the fuel supply to the SOFC is greater and the cell voltage is also higher, which provides greater cell power. A higher TIT also increases the gas turbine power. Thus, the total system power in-

creases with increasing TIT. The increase of the gas turbine power with increasing TIT is more evident than that of the SOFC power. Thus, the resulting power ratio decreases with increasing TIT. The system efficiency is predicted to be over 60% and increases with increasing TIT. Even though these tendencies are common for the two layouts, there are a few different quantitative aspects between the two layouts. For a given TIT, the ambient pressure system can achieve greater system power than the pressurized system, mainly because of the larger SOFC power (see the greater power ratio), which is attributed to the higher cell temperature. The power ratio ranges from 9 to 12 for the ambient pressure system, while that of the pressurized system ranges from 6 to 7.5. The higher FCT leads to a greater temperature difference at the cell (thus greater fuel supply to the cell) as well as a higher cell voltage. Both effects contribute to the larger SOFC power. Of course, a larger SOFC power requires a greater cell size because the current density is assumed to be constant.

Even though the pressurized system has smaller power capacity, it exhibits higher system efficiency (2 percent point on the average) than the ambient pressure system for all conditions. This means that the fuel energy is more effectively utilized in the pressurized system. In the ambient pressure system, the average temperature difference at the cell is about 40°C higher than that of the pressurized system. Consequently, the ambient pressure system may have greater thermal load in the SOFC stack, while having a greater power capacity than the pressurized system.

The difference in the system efficiency between the two layouts can be more easily explained by the exergy analysis. Fig. 3 demonstrates exergy breakdowns for the two layouts. Exergy destructions and losses are shown as the percentage of fuel exergy input. Here, 'Fuel cell' means the entire fuel cell composed of the fuel cell stack and the internal reformer. Even though the detailed loss distribution varies among different design conditions, the largest source of exergy destruction (or loss) is the exhaust gas. The second largest source of exergy destruction is the fuel cell stack including the internal reformer. Afterburner is

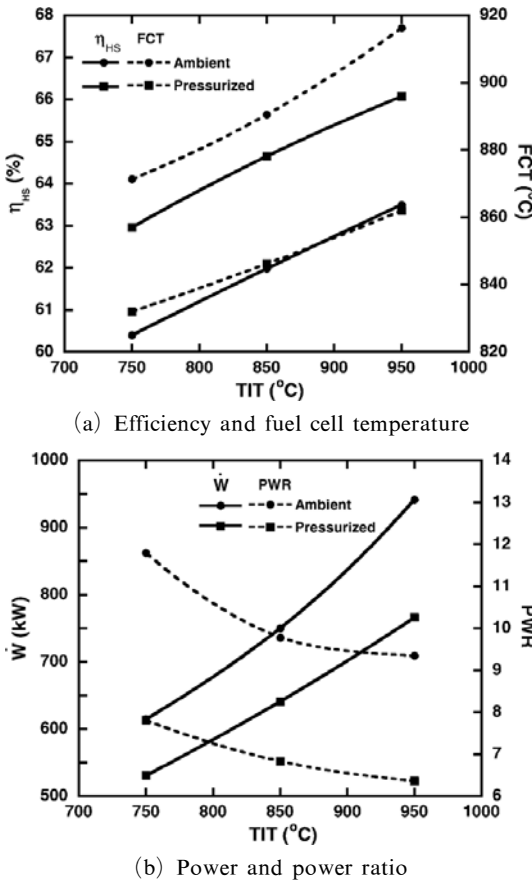


Fig. 2 Design performance under a relaxed constraint on the cell

also one of the large destruction sources because of the highly irreversible nature of the combustion process. Another important source of exergy destruction is the recuperator. Total exergy destruction is inversely proportional to the system efficiency. The efficiency discrepancy between the two layouts is mostly due to the differences in the exhaust exergy loss and the exergy destruction at the recuperator. Both values are higher for the ambient pressure system. In the ambient pressure system, the exergy destruction at the recuperator

is larger than the pressurized system because the temperature difference between the hot gas and the air is relatively large. Moreover, the exhaust gas temperature is still high, resulting in large exhaust loss. On the other hand, the energy of the high temperature gas from the fuel cell is more effectively utilized in the pressurized system by recovering the energy at the turbine and the recuperator.

4.2 Restricted constraint on the cell

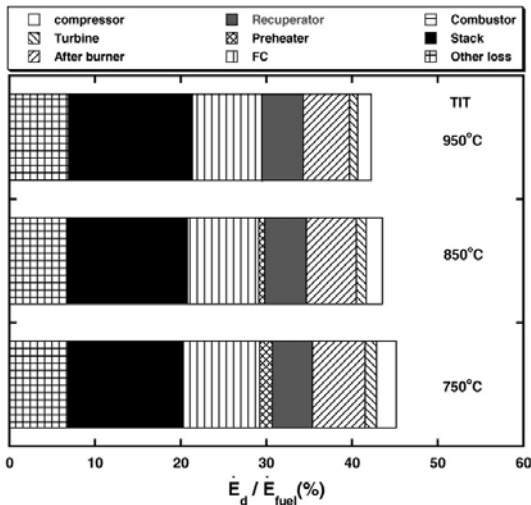
This section presents results for the analysis with a restricted design constraint on the fuel cell. The constraint is that the temperature difference at the cell (ΔT_{cell}) must be smaller than a maximum allowable value. This allowable temperature difference may depend on material capability and thermal management technology. A value of 200°C is given in this study. Three major parameters (fuel cell temperature, temperature difference at the cell and turbine inlet temperature) must be satisfied simultaneously. To meet this restricted requirement, the dotted lines of Fig. 1 are introduced. For both layouts, additional fuel is supplied to increase the TIT when it tends to decrease. The ratio of the additional fuel supply is defined as follows :

$$FR = \frac{\dot{m}_{f,add}}{\dot{m}_{f,total}} \tag{19}$$

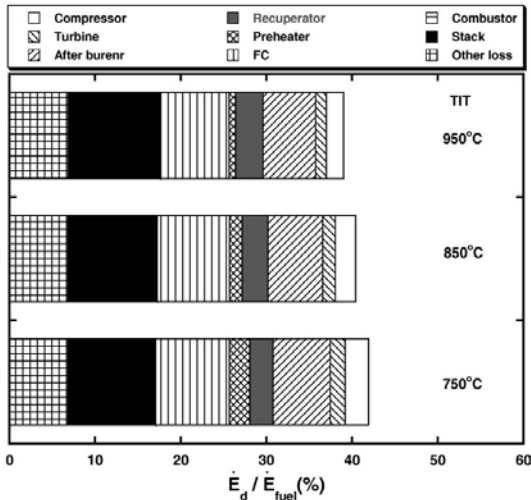
The air bypass functions differently in the two layouts. In the ambient pressure system, if the temperature difference at the cell tends to be less than the given value (i.e. if the cell inlet temperature tends to decrease under the set value), some of the inlet air is bypassed from the system inlet line to the SOFC. In the pressurized system, some portion of the recuperator exit air is bypassed to the turbine side if the TIT tends to be too high. The air bypass ratio is defined as follows :

$$AR = \frac{\dot{m}_{a,bypass}}{\dot{m}_{a,total}} \tag{20}$$

Given ΔT_{cell} , the performances of the two layouts are estimated for various combinations of FCT and TIT. Fig. 4 presents the additional fuel supply ratio and the air bypass ratio of the am-



(a) Ambient pressure system

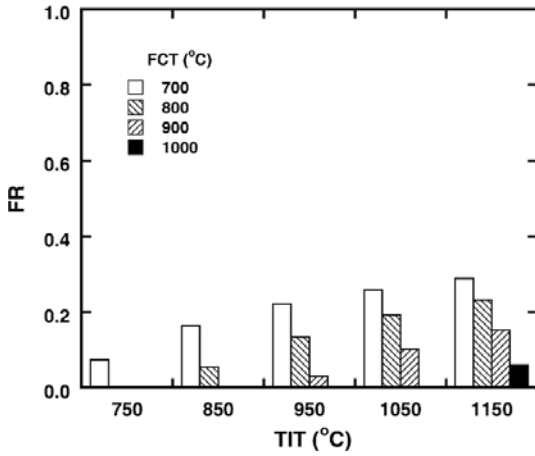


(b) Pressurized system

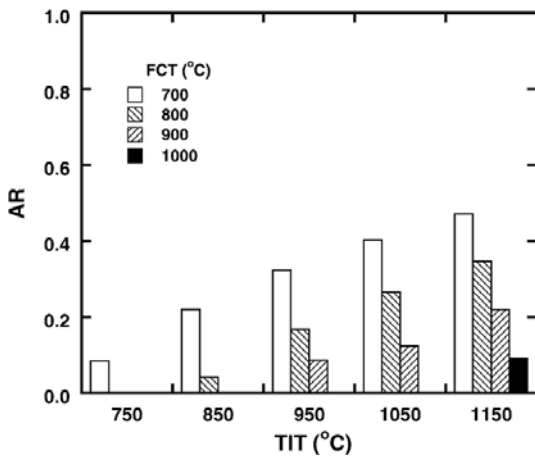
Fig. 3 Exergy destructions under a relaxed constraint on the cell

bient pressure system. For a given FCT, when the TIT increases, the additional fuel supply must be increased. As the additional fuel supply ratio increases, the turbine exit temperature increases. This tends to increase the cell inlet temperature, and thus the temperature difference at the cell reduces. If the turbine exit temperature is too high, the gas does not need to be preheated; moreover, some air needs to be supplied directly to the SOFC to satisfy the cell inlet temperature (i.e. temperature difference at the cell). Therefore, the air bypass ratio is proportional to the additional fuel supply ratio. Fig. 5 shows the additional fuel supply ratio and the air bypass ratio of the pres-

surized system. The tendency of variation of the additional fuel supply ratio is similar to that of the ambient pressure system. However, the variation of the air bypass ratio is completely different. In the pressurized system, the purpose of the air bypass is to reduce the turbine inlet temperature when it tends to increase, which is just the opposite function of the additional fuel supply. Thus, air should be bypassed to the turbine side if the design TIT is low enough. The amount of the air bypass increases as the TIT decreases. Consequently, either the air bypass or the additional fuel supply may be executed in the pressurized system.

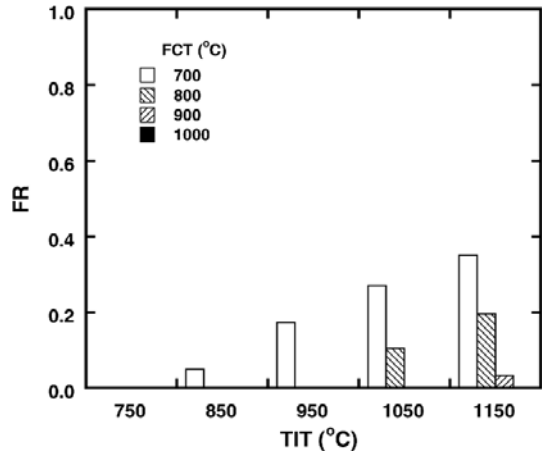


(a) Additional fuel supply ratio

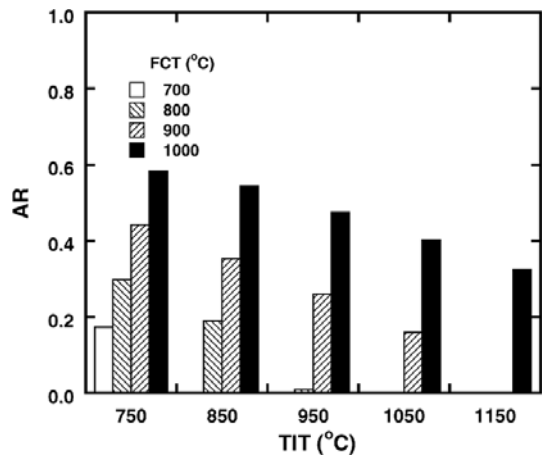


(b) Air bypass ratio

Fig. 4 Additional fuel supply ratio and air bypass ratio of the ambient pressure system under a restricted design constraint on the cell



(a) Additional fuel supply ratio



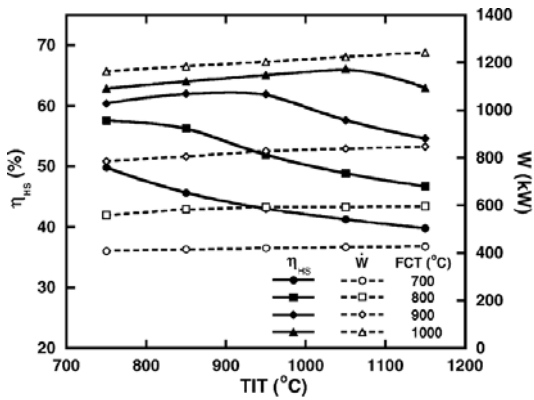
(b) Air bypass ratio

Fig. 5 Additional fuel supply ratio and air bypass ratio of the pressurized system under a restricted design constraint on the cell

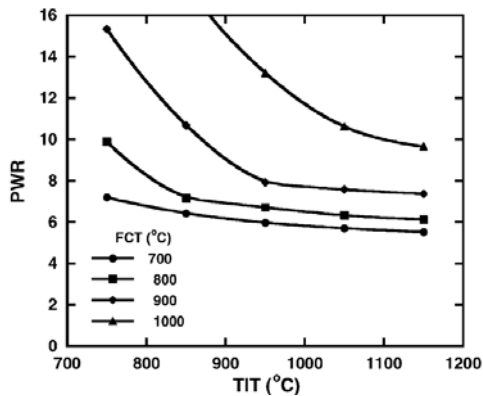
System performances are shown in Figs. 6 and 7 for the ambient pressure system and the pressurized system, respectively. For a given FCT, increasing TIT leads to larger power, which is true for both layouts. System efficiency increases to an optimal point, after which it decreases. The optimal TIT increases as the FCT increases. The maximum efficiency point almost corresponds to the design condition where the additional fuel supply begins (see Figs. 4 and 5). In the ambient pressure system, the SOFC power remains nearly constant for a given FCT because air flow rate supplied to the SOFC is almost constant regardless of the air bypass at the system inlet. The slight increase of the total system power with increasing TIT is due to the increase of gas turbine power. As a result, the power ratio decreases with increasing TIT for a given FCT. In the pressurized

system, the SOFC power shows a different trend. Even though the total inlet air flow rate is fixed, the SOFC power reduces if some air is bypassed to the turbine side. If FCT is sufficiently high (1000°C for example), air should be bypassed as TIT decreases, and this bypassing reduces the SOFC power. At sufficiently low FCT (700°C for example), air does not need to be bypassed for a wide TIT range, where the SOFC power is almost constant. The power ratio of the pressurized system is smaller than that of the ambient pressure system.

For all design conditions, the efficiency of the pressurized system is higher than that of the ambient pressure system. This trend is similar to that of the previous section. However, the efficiency gap between the two layouts is greater in the case under a restricted constraint, as presented in this

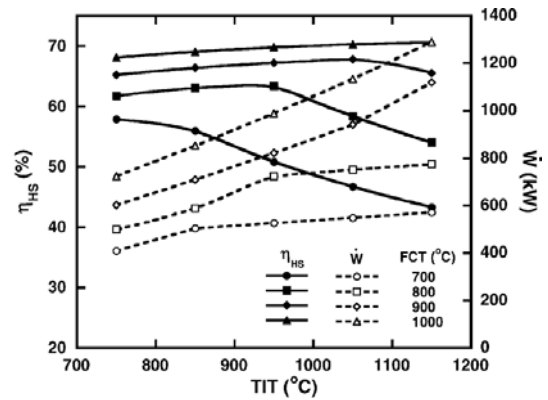


(a) Efficiency and power

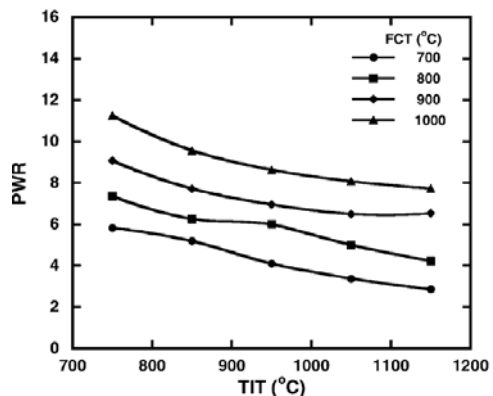


(b) Power ratio

Fig. 6 Design performance of the ambient pressure system under a restricted constraint on the cell



(a) Efficiency and power

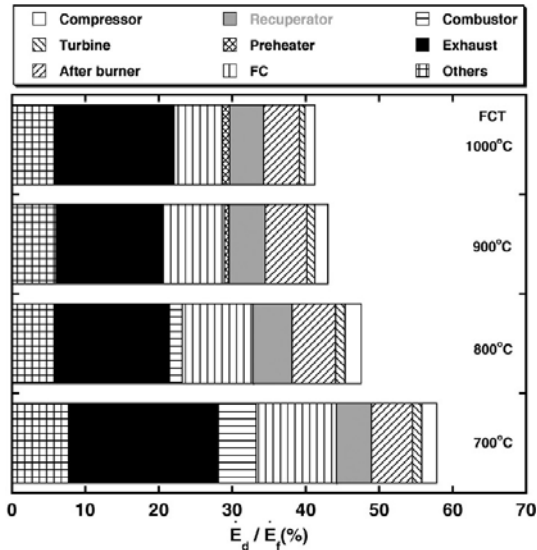


(b) Power ratio

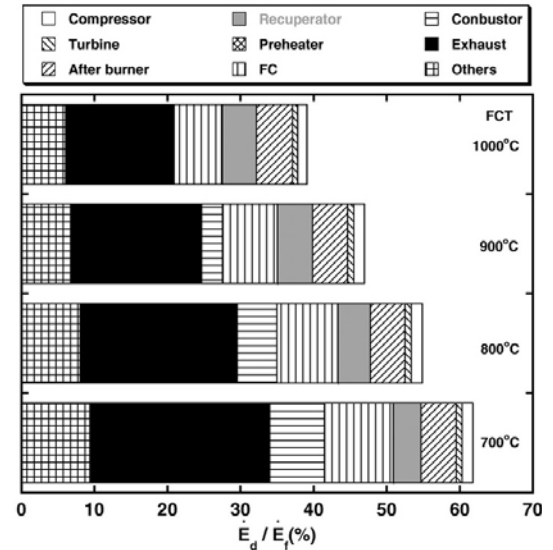
Fig. 7 Design performance of the pressurized system under a restricted constraint on the cell

section. As we have seen in Fig. 2 of the relaxed design constraint, the efficiency gap is less than two percent points. However, the efficiency difference under the restricted constraint is far larger than that of Fig. 2. This means that as the restriction on the cell design becomes severe, the efficiency advantage of the pressurized system becomes more evident. The pressurized system provides

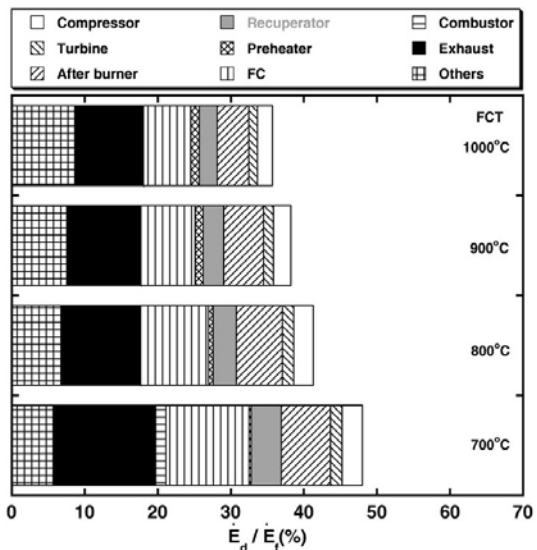
60% system efficiency with the fuel cell temperature roughly over 800°C in the pressurized system, while the ambient pressure system requires a far higher cell temperature (900°C). Figs. 8 and 9 illustrates examples of exergy breakdown for TIT of 850°C and 1050°C. In general, a higher FCT reduces most of the exergy destructions, thus results in higher efficiency. This can be seen from



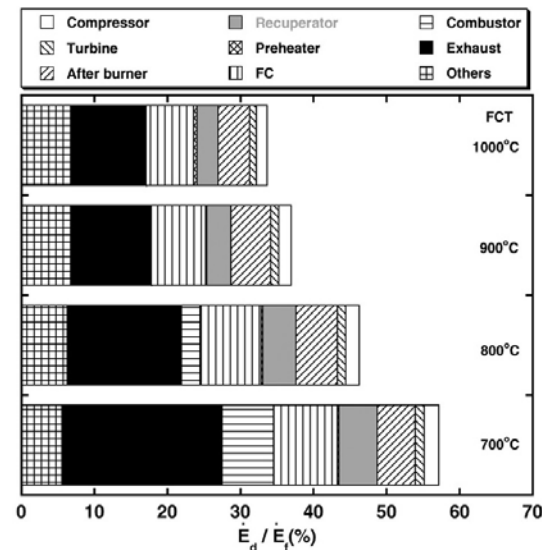
(a) Ambient pressure system



(a) Ambient pressure system



(b) Pressurized system



(b) Pressurized system

Fig. 8 Exergy destructions for the restricted design condition on the cell for TIT of 850°C

Fig. 9 Exergy destructions for the restricted design condition on the cell for TIT of 1050°C

results for a given TIT. The superior efficiency of the pressurized system can be explained by the smaller exergy destructions and losses. In particular, far smaller exhaust loss and recuperator destruction of the pressurized system contributes to the higher system efficiency. This result reconfirms the fact that the pressurized system utilizes the energy of the high temperature gas more effectively. Comparison between results in Figs. 8 and 9 also shows that the efficiency variation with TIT change (Figs. 6 and 7) follows the trend of exergy loss variation. For example, at low FCT's of both systems, increasing TIT increases exergy destructions and losses, which matches the efficiency reduction with increasing TIT shown in Figs. 6 and 7. In particular, increasing TIT at low FCT's causes large increases of the exhaust exergy loss and the exergy destruction at the combustor where additional fuel is added.

5. Conclusions

Design performances of two layouts of SOFC/GT hybrid systems, with the major difference being the operating pressure of the SOFC, are comparatively analyzed. The following summarizes the results.

- (1) Power share of the SOFC is greater in the ambient pressure system for all design conditions.
- (2) If not restricted, the cell temperature needs to be designed higher and the temperature difference at the cell stack is greater in the ambient pressure system.
- (3) Under any design constraint, the pressurized hybrid system exhibits higher efficiency than the ambient pressure system. This is mainly due to the more effective utilization of the energy of the high temperature gas from the fuel cell, which is demonstrated by the relatively smaller exhaust exergy loss as well as less exergy destructions at components such as heat exchangers.
- (4) By modulating the additional fuel supply and air bypass, three main design temperature parameters such as fuel cell temperature, temperature difference at the cell and turbine inlet temperature can be set simultaneously for both lay-

outs. Under the restricted constraint, the efficiency advantage of the pressurized system is manifested; 60% system efficiency can be achieved for fuel cell temperature roughly over 800°C in the pressurized system, but the ambient pressure system requires higher cell temperatures (900°C).

Acknowledgments

This work was supported by the Korea Research Foundation Grant funded by the Korean Government (MOEHRD) (KRF-2005-041-D00156).

References

- Agnew, G. D., Bozzolo, M., Moritz, R. R. and Berenyi, S., 2005, "The Design and Integration of the Rolls-Royce Fuel Cell Systems 1MW SOFC," ASME paper GT2005-69122.
- Aspen Technology, 2004, AspenOne HYSYS, ver 2004.02.
- Chan, S. H., Low, C. F. and Ding, O. L., 2002, "Energy and Exergy Analysis of Simple Solid-Oxide Fuel-Cell Power Systems," *Journal of Power Sources*, Vol. 103, pp. 188~200.
- EG & G Services Parson, Inc., 2000, *Fuel Cell Handbook, 5th Ed*, U.S. Department of Energy.
- Larminie, J. and Dicks, A., 2000, *Fuel Cell Systems Explained*, John Wiley & Sons, Ltd..
- Liese, E. A. and Gemmen, R. S., 2003, "Performance Comparison of Internal Reforming Against External Reforming In a SOFC, Gas Turbine Hybrid System," ASME paper GT 2003-38566.
- Massardo, A. F. and Lubelli, F., 2000, "Internal Reforming Solid Oxide Fuel Cell-Gas Turbine Combined Cycle (IRSOFC-GT), Part A: Cell Model and Cycle Thermodynamic Analysis," *Trans. ASME, Journal of Engineering for Gas Turbines and Power*, Vol. 122, pp. 27~35.
- Massardo, A. F. and Magistri, L., 2001, "Internal Reforming Solid Oxide Fuel Cell-Gas Turbine Combined Cycles (IRSOFC-GT), Part B: Exergy and Thermo-economic Analyses," ASME paper 2001-GT-0380.
- Moran, M. J. and Sciubba, E., 1994, "Exergy Analysis: Principles and Practice," *Trans. ASME*,

Journal of Engineering for Gas Turbines and Power, Vol. 116, pp. 285~290.

Moran, M. J. and Shapiro, H. N., 2004, *Fundamentals of Engineering Thermodynamics*, 5th Ed., John Wiley & Sons, Ltd..

Oh, K. S. and Kim, T. S., 2006, "Performance Analysis on Various System Layouts for the Combination of an Ambient Pressure Molten Carbonate Fuel Cell and a Gas Turbine," *Journal of Power Sources*, Vol. 158, pp. 455~463.

Singhal, S. C. and Kendall, K., 2003, *High Temperature Solid Oxide Fuel Cells : Fundamentals, Design and Applications*, Elsevier Ltd.

Song, T. W., Sohn, J. L., Kim, J. H., Kim, T. S., Ro, S. T. and Suzuki, K., 2005, "Performance Analysis of a Solid Oxide Fuel Cell/Micro Gas Turbine Hybrid Power System Based on a Quasi-Two Dimensional Model," *Journal of Power Sources*, Vol. 142, pp. 30~42.

Veyo, S. E., Lundberg, W. L., Vora, S. D. and Litzinger, K. P., 2003, "Tubular SOFC Hybrid Power System Status," ASME paper GT2003-38943.

White, D. J., 1999, "Hybrid Gas Turbine and Fuel Cell Systems in Perspective Review," ASME paper 99-GT-419.

Yang, W. J., Kim, T. S. and Kim, J. H., 2005, "Comparative Performance Analysis of Pressurized Solid Oxide Fuel Cell/Gas Turbine Hybrid Systems Considering Different Cell Inlet Preheating Methods," *Trans. of KSME B*, Vol. 29, No. 6, pp. 722~729.

Yang, W. J., Kim, T. S., Kim, J. H., Sohn, J. L. and Ro, S. T., 2006, "Design Performance Analysis of Pressurized Solid Oxide Fuel Cell/Gas Turbine Hybrid Systems Considering Temperature Constraints," *Journal of Power Sources*, Vol. 160, pp. 462~473.